

Model Error Budgets

Hugh C. Briggs*

Jet Propulsion Laboratory, California Institute of Technology, Pasadena, CA 91109

An error budget is a commonly used tool in design of complex aerospace systems. It represents system performance requirements in terms of allowable errors and flows these down through a hierarchical structure to lower assemblies and components. The requirements may simply be “allocated” based upon heuristics or experience, or they may be designed through use of physics-based models. This paper presents a basis for developing an error budget for models of the system, as opposed to the system itself. The need for model error budgets arises when system models are a principle design agent as is increasingly more common for poorly testable high performance space systems.

I. Objective

Projects may be particularly sensitive to the quality of models for a variety of reasons. Model performance requirements might be levied in an attempt to bound the project’s risk. For example, a recent modeling requirement was stated:

The difference between experimental measurement and analytical model prediction of OPD (rms) over 1 hour period shall be less than 30% or 30 pm, whichever is greater.

This requirement constrains the difference between model and experiment and might be better termed “total uncertainty” rather than “model uncertainty.”¹⁶ The contributions from the model might be broken down by various schemes, but one is data uncertainty, solution verification, parametric uncertainty, and model form uncertainty.^{17, 19}

The modelers can invest the given resources in many areas such as finer meshes, higher precision algorithms, or smaller time steps. An error budget could be an investment guide, directing effort to portions of the model with high error budget impact, as well as providing error partitioning to assure that the goal is achieved.

The fields of stochastic analysis, sensitivity analysis and optimization have made significant progress. This paper isn’t about those areas, per se, but rather their application to a larger problem. Large multidisciplinary models, as are common in design of controlled optical systems, are expensive to build and verify. Project leaders have difficulty knowing which part of the model, which discipline or which verification test will prove to be the critical link in the results chain. Similarly, if the modeling activity has a precision requirement, it can be difficult to know which mesh, which load or which material property is most important. Clearly, we have to tools to answer these questions individually. This paper puts this into a framework for organizing the choices, identifying weights and priorities, and providing a sound basis for investment decisions. When enough money is available to only tackle the top two or three driving issues, such a decision strategy is essential.

II. Background

This paper addresses a multidisciplinary problem in high performance space-borne optical systems. The analytical process is straight forward, but expensive, and has been characterized as a “bucket brigade.”^{1,2} It is expected to be the analytical basis for design approval of a system too large to adequately test before flight. Significant concern exists over the sensitivity of results to unknown material parameters as well as poorly understood physics of mechanical systems in 0g. These are not phenomenologically complex systems, such as ballistics penetration,^{14,15} denotation of high explosives due to impact,¹⁷ or a weapon system in a fire where the issue is probability of Loss of Assured Safety.¹⁹

Sensitivity factors are the essence of selecting weights in an informed error budget. Optimization activities have invested heavily in analytical derivatives in these equations for a number of years.

Analysis of stochastic or uncertain systems is a related area which has undergone significant transformation in recent years. While the modeling methods here are deterministic, these techniques can be used to predict the range

* Develop Hardware Products Process Engineer, M/S 158-224, and Associate Fellow.

of results given variations of parameters such as a material property. In themselves, these methods provide little help at this point in determining the structure of an error budget or the appropriate weights.

Sensitivity of fields (eg displacements, stresses, or temperatures) is used in various applications including optimization and uncertainty propagation. Loeven, et al, use sensitivity analysis in fluid-structure interactions and report the use of sensitivity analysis in flow problems.¹⁰ Common methods for computing the sensitivities are, among others, finite differencing, the complex step method, automatic differentiation, and the continuous sensitivity equation approach. HCB: look up references from AIAA short course, or use the ones from ref 10.

In large, multidisciplinary problems such as this, many factors are dependent upon the size of the mesh. Most notable is the trade between solution accuracy and solution time, but there is also significant cost in building the meshes and moving dense solutions between discipline domains. Provided the coarsest mesh is in the asymptotic regime of convergence where the truncation error dominates the overall numerical error, multiple approaches exist to verify the rate of convergence in successively refined meshes and estimate an extrapolation of the continuous solution.^{4, 9} The Grid Convergence Index was developed by Roache to provide a standardized metric that is independent of the order of the numerical method and refinement strategy.^{7, 8}

There are a modest number of physical properties in complex systems that have both a significant impact on performance and have uncertain or spatially varying values. Even when characteristic data about the property is available, incorporation into the numerical analysis can lead to costly, large and complex models and significantly extended solution times. Ghanem, et al, have established a multiple part method to generate spatially varying material property decks to model epoxy foam.⁶ They use stochastic spatial interpolation to handle imprecise and spatially scarce information to provide “an indication as to the suitability of the experimental effort and its sufficiency towards a validation exercise.” Sarkar and Ghanem similarly use Polynomial Chaos expansion, concepts of matrix calculus and the Kronecker products to develop the sensitivity of stochastic model outputs to the random scatter in stochastic input parameters.¹⁸

Uncertainty in the system may be broadly divided into two categories.^{11, 19} The first type is due to the inherent variability in the system parameters and is often referred to as *aleatoric uncertainty*. The second type of uncertainty is due to the lack of knowledge regarding a system, often referred to as *epistemic uncertainty*. Epistemic uncertainty does not directly depend on system parameters and is often modeled using a non-parametric approach. Adhikari has shown how to characterize system dynamic frequency response functions using Random Matrix Theory.¹¹ Under simple realistic constraints, the probability density function of the system dynamics matrix and its inverse are known to be readily computed via Wishart random matrices. In an example problem of a cantilever plate whose finite element model had 429 degrees of freedom, Adhikari characterized the only uncertainty information as a percentage of the mass matrix and obtained good agreement to a higher fidelity Monte Carlo simulation. The closed form expressions for the system matrix inverse provide an important simplification of the analysis.

Test data has been used quite successfully to estimate system parameters as well as to provide update or corrective information to improve models. Fraccone, et al, demonstrate a method to identify faulty sensors in a test apparatus, as well as extrapolation techniques to fill in for a spatially sparse sensor field.⁵ Their goal is to develop a statistically rigorous procedure for incorporation of experimental information into the system model.

It is common with exotic materials or regular materials under extreme temperatures to have poorly defined material properties. Huysse et al show how to incorporate rough interval data and expert opinion so that the potential gain from additional measurements can be assessed.¹² Of course, the goal of a verification and validation program is to establish confidence, or credibility, in model predictions through the logical combination of focused laboratory experimentation, hierarchical model building, and uncertainty quantification.¹³ Such a priori planning needs to reflect the important interaction between the modeler and the experimenter that must occur to ensure that the measured data is needed, relevant and accurate.^{14, 15}

Each of these addresses a relevant area of the current problem. They provide sophisticated techniques to quantify several needed aspects. The current work focuses, instead, on the higher level structure of the integrated error budget. With this understood, in time, individual components can be refined through such techniques.

III. Integrated Modeling

Integrated system models predict performance in mission relevant terms. Optical systems might have metrics such as wavefront error, wavefront tilt, and optical path difference (OPD). These metrics might be perturbed by structural dynamics, controller errors, or thermal distortions of the support structure. A typical integrated modeling flow for thermally induced deformation of optical structures is depicted in Fig. 1.^{2, 3}

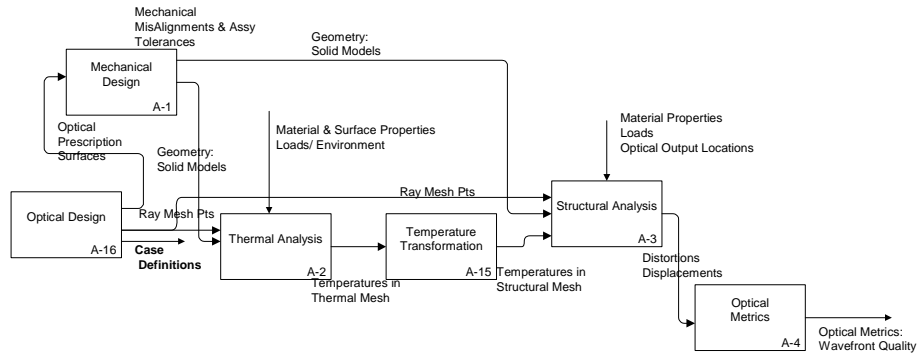


Figure 1. Integrated Modeling Process

This integrated, multidisciplinary analysis is driven by temperatures that represent the in-space operational conditions during a maneuver. The temperatures computed in the thermal problem are mapped from the thermal grid to the structural grid and then applied as thermal strains to the structural model. The mirror face distortions are exported and the optical metrics are computed in stand alone optical design tools.

The integrated modeling problem of Lindensmith, et. al.³ and Briggs, et. al.² is summarized in the following and will be used as the example problem in later sections.

The CAD geometry was used to ensure that the thermal, structures, and optical models would all be based on a common solid model and that all models would occupy the same positions in space. Fig. 2, Test Chamber Models in Teamcenter Engineering, shows the design CAD models that were the basis for the analysis.

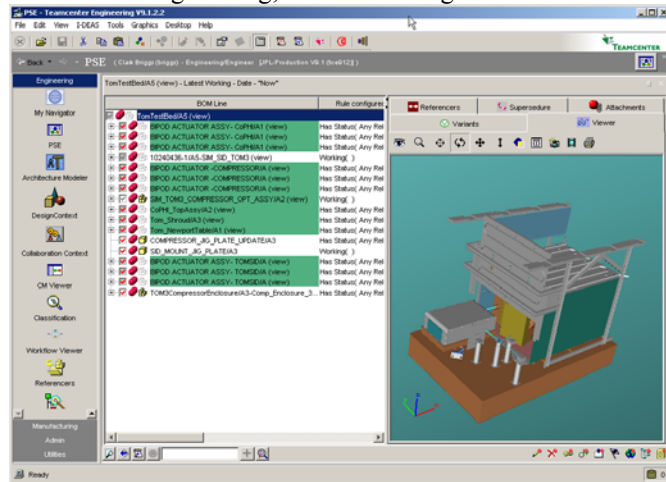


Figure 2. Test Chamber Models in Teamcenter Engineering

The thermal model is very complex and is designed to resolve temperature spatial gradient changes over time. It has an optimized mesh density on the mirror and closely matched geometry and part mass. Outer MLI layer elements are explicitly modeled including MLI cutouts for monopods and actuators. The fine scale thermal model had 13,500 radiation elements and 23,800 mass and conduction elements. The thermal model is shown in Fig. 3 and an exploded view of the siderostat (SID) thermal model is in Fig. 4.

The facility thermal model, shown in Fig. 5, is a simplified model used for design of the test program procedures. The facility model geometry is very simplified compared to the fine model and does not contain siderostat monopod, thermal can bipod geometry, or actuators, using thermal links instead.

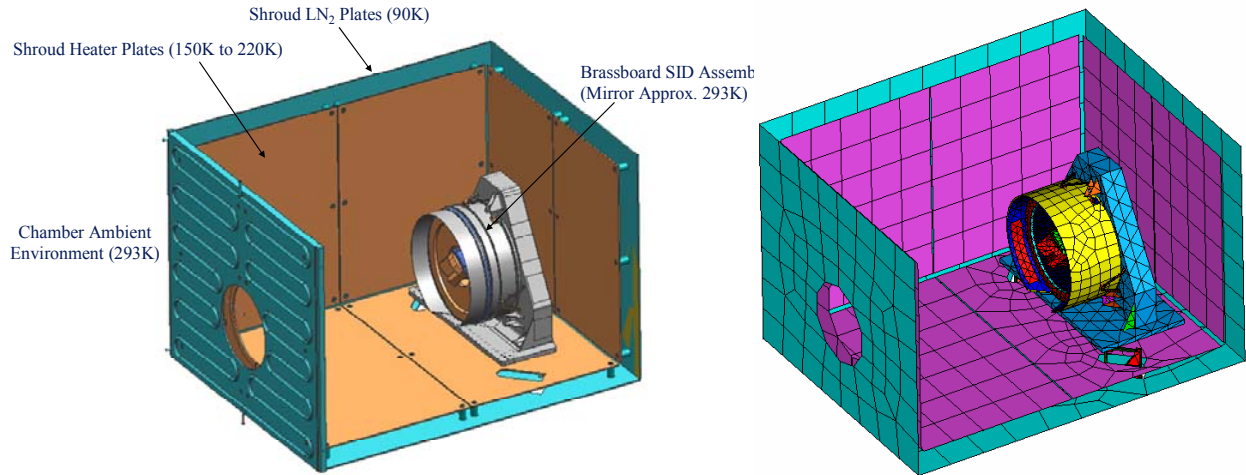


Figure 3. Fine Scale Thermal Model

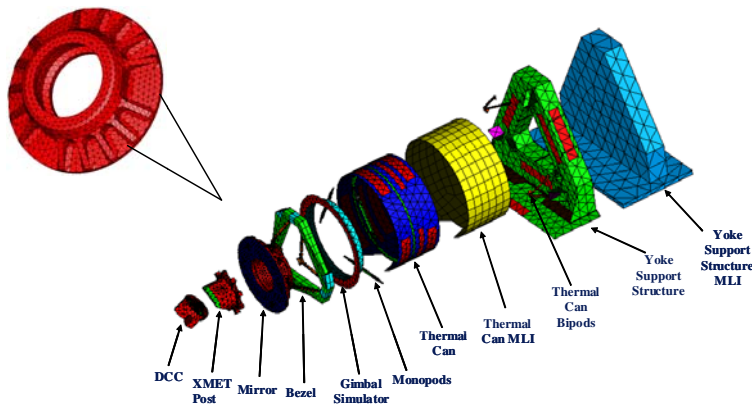


Figure 4. SID Fine Scale Thermal Model – Exploded View

positions and orientations of the optical elements. The optical layout is illustrated in Fig. 7. The optical models used in this integrated analysis were based upon geometric optics assumptions and were typically expressed as sensitivities to be multiplied by the displacements of the structural solution. The mission optical metric modeled in the tests and analyses was the path length difference between the science light path reflecting off of the siderostat mirror and the internal metrology light path which hits the Double Corner Cube (DCC) in the middle of the mirror.

The structural models were developed from the hardware CAD models and were designed to map temperatures from the thermal models. Fig. 6 shows the structural model developed for the SID. This model has 47,000 elements and 168,000 nodes. The actuator mechanisms were modeled as elastic beams. The model also contained the bipod supports which in turn were connected with rigid elements to a ground point.

The optical models used the system optical prescription to evaluate the OPD metric under small perturbations to the

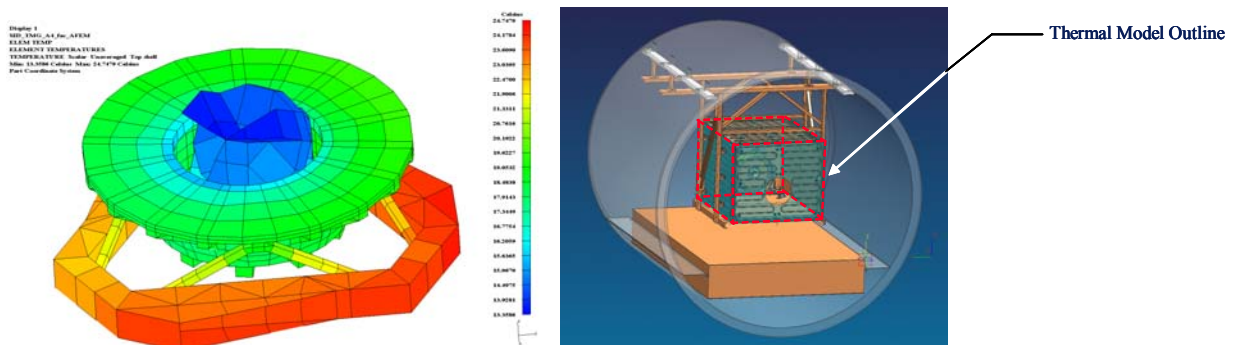


Figure 5. Facility-Level Thermal Model

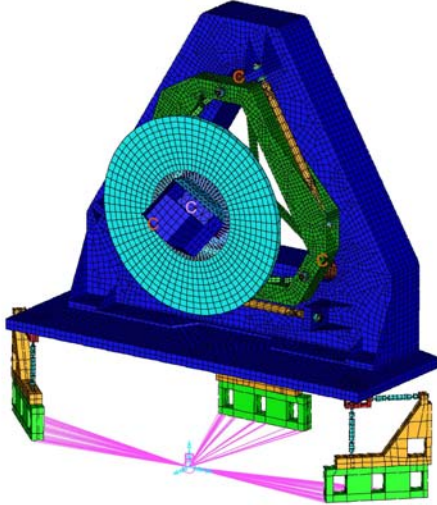


Figure 6. Fine Scale Structural Model

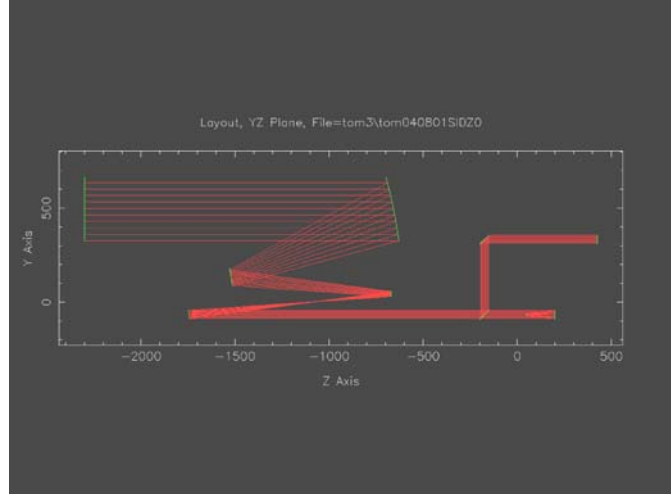


Figure 7. Optical Model

IV. Error Sources In Models

Large, complex, multi-disciplinary models contain many components and their utilization requires many steps. Clearly, errors could be present in each. Several structural analysis error sources are listed in Table 1, while similar error sources for thermal modeling are listed in Table 2.

Element Behavior Approximations
Mesh Approximates Spatial Behavior
Element Type Transitions
Modeling Abstraction Omits Mass & Stiffness
Part Connection Abstraction Impacts Stiffness
Joint Modeling Approximations
Use of Nominal Material Properties
Use of Measured Material Properties & Their Uncertainties
Static Assumption Omits Vibration Effects on Optical Performance
Approximations in Local Normal at Ray Point
Approximation of Deformed Normal Tip & Tilt
Support Modeling Impacts Stiffness & Load Distribution

Table 1. Structural Analysis Error Sources

Mesh Approximates Temperature Field Spatial Variations
Part Connection Modeling Impacts Thermal Conduction
Use of Nominal Material Properties
Use of Measured Material Properties & Their Uncertainties
Geometry Approximations of Mass, View Factors
Modeling Chamber Boundary Conditions
Mesh Differences & Interpolation Algorithm in Temperature Mapping
Assigning Temperature Fields to Equivalent Structural Surfaces/Volumes
Modeling DCC and Mapping Temperatures to Structural DCC Model
MLI Placement and Properties
Modeling Heater Placement & Input Effectiveness
Modeling Boundary Cold Plate Spatial Variations and Load Effectiveness

Table 2. Thermal Analysis Error Sources

These will be discussed briefly in the following. Other potential sources of error include the numerical solution tolerance, precision of the routines, and error in manual data manipulation. The discussion illustrates a few of these with the goal of shedding light on the modelers' investment concerns.

The mirrors are mounted on bipods with cross-blade flexures integrally machined into both ends. Although these supports are designed to exert minimal bending loads on the mirror, the residual moments cause measurable deformation at these precisions. The majority of the support was modeled with volume elements while the thin blades were modeled as bending plates. In contrast, the bond layer between the mirror and the bipods was modeled with a thin layer of volume elements to capture thermal expansion, after a short study of the meshing effects. These are both examples that trade off degrees of freedom for simplification.

In thermal modeling, prior technology development studies had demonstrated that temporal thermal results depended significantly on capturing better than 99% of the thermal volume in the mirrors. This led to high density thermal conduction meshes. Similarly, since the primary heat transfer mechanism is radiative transport, the radiation view factors needed to be captured better than 99%. This led to unprecedented high density meshes on much of the mirror surfaces.

Mirror performance was known from earlier technology studies to be very sensitivity to the coefficient of thermal expansion. Published manufacturer's values of this property showed wide variations. Comparison to initial test results showed poor model performance and investigation questioned the values of the coefficient of thermal expansion for the test article. The prior data as well as new measurements for the boule showed significant spatial variation both through and across the face of the mirror. These were ultimately incorporated via a large material property table.

This multidisciplinary model includes different meshes for structural deformation, temperature and the optical wavefront. The interpolation of the temperature field into the structural grid was studied carefully. The computations were scrubbed of single precision steps, a dense thermal grid was used, and all manual transfer and formatting steps were scrutinized. Two optical grids were used. A coarse grid that matched the path length sensor spots was used for the geometric optics model and a large 1024x1024 grid was used for the Fourier optics diffraction model. Both used the structural model surface normal displacement interpolated in the structural grid.

The total size of the models was known to be a limitation on the solution accuracy, solution wall clock time and the manual processing of the data sets between models. The most limiting of these was the thermal solution time and the conversion of the temperatures to structural loads. The thermal model was expected to be challenging and the largest known by a substantial margin. This constrained the model fidelity in terms of spatial mesh and time step size. A simplified facility thermal model was used to guide construction of the thermal shrouds and to estimate key radiation properties based on facility check out runs.

V. An Allocated Error Budget

An initial budget might consider error sources to be equally weighted producing an error budget such as Fig. 8.

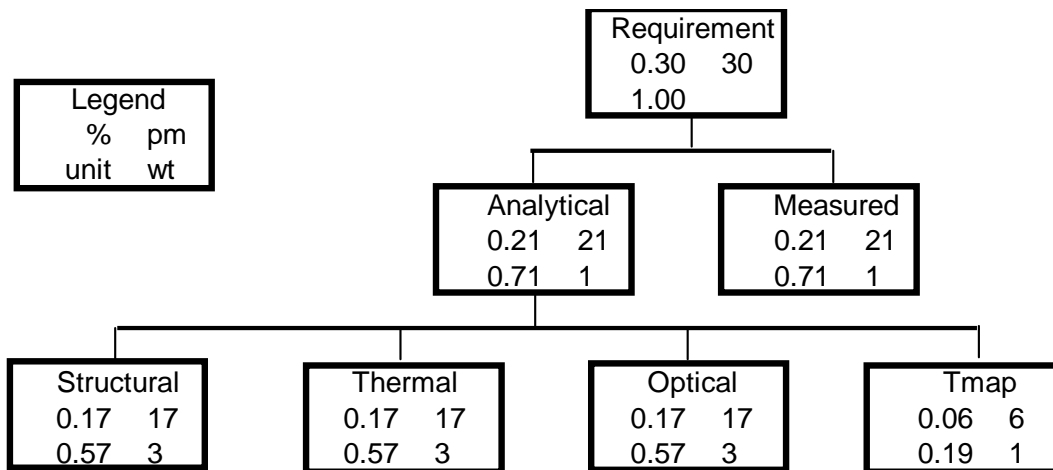


Figure 8. Equally Weighted Error Allocation

In this case, the allowed error is equally allocated between analysis and the experiment and, within the analysis, the error is equally allocated to each of the discipline analysis steps.

The requirement is formulated as a difference between the experimental measurement and the analytical result, without any means to apply the experimental uncertainty. The experiment setup provided only a small set of

precision temperature sensors and no deformation sensors. The optical path measurement was very noisy because of the extremely low deformation levels and extensive time averaging required. In practice, the thermal excitation had to be raised above mission requirements to achieve usable measurements.^{21, 3}

The error allocation in Fig. 8 presumes the goal of estimating the actual system performance, with balanced inputs from two estimates. Better insight might be available by plotting both the analysis and the experimental results versus time, along with their error bars.²⁰

As illustrated in the discussion above concerning error sources, there are many potential sources in each discipline's model. Many of them are independent of factors in other disciplines. The fourth allocation in Fig. 8 reflects the mapping or interpolation of temperature results in the thermal grid to the loads in the structural grid. In comparison, the lower weight is justified based on the much simpler and better understood process.

This error allocation provides little concrete guidance to investment in any of the disciplines, beyond they each appear to be equally challenging. Other than a brief study of the bond pads, the structural team proceeded to build a high quality model, likely capable of picometer thermal distortions, within the given staffing and calendar time. The thermal team, guided by the opportunity to use early temperature measurements, calibrated parameters with the facility model and then constructed a fine-scale model that was limited by solution time.

This error allocation scheme proved to be entirely unacceptable to guiding decisions because the numerical relationships between the discipline models are well known. There is great intuitive understanding that an error in a driving temperature causes a certain amount of deformation and therefore a certain amount of OPD error.

Any reasonable error budget must be informed by the physical processes to reflect the cascading effects.

VI. A Physics-Based Error Budget

For integrated modeling, the error budget can reflect the sequence of discipline solutions in the budget structure. See Fig. 9 where, starting from the bottom, the operational scenario drives the thermal problem which contributes to the structural problem, etc. In this figure, the branch weights have not been assigned and would be based on sensitivity studies for a particular problem.

There are several the difficult issues associated with this error budget form despite its logical appeal. The following illustrates simple techniques to formulate relevant branch weights before tackling the bigger problem of formulating a single integrated budget.

A significant concern from the beginning was that the extreme precision required would drive the mesh densities up too high to be affordable to make and compute with. To explore the impact of mesh density on computed results simple numerical trials were conducted. The mirror plays the central role in system performance here. It drives the first order optical wave front metric via reflection off its front face. The distortion of the reflective face is driven by thermal expansion and through-the-thickness temperature gradients were known from early technology experiments to be the primary driver. The as-designed temperature field is to be very nearly uniform, with low wave number spatial variations.

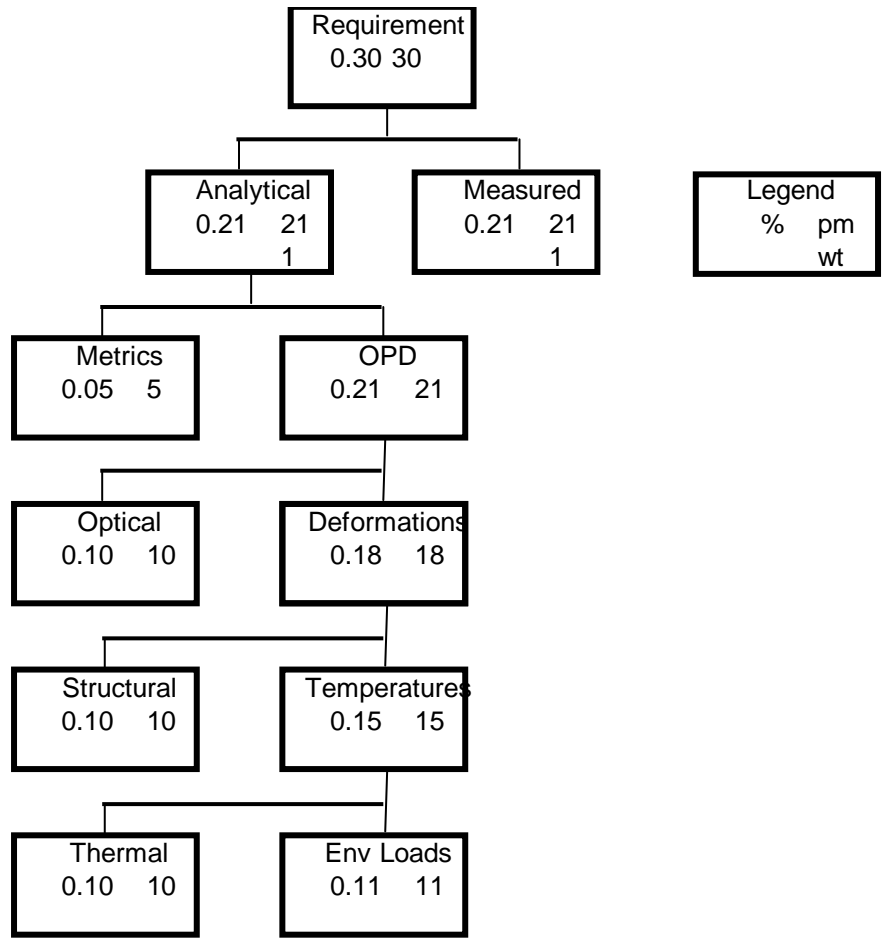


Figure 9. A Physics-Based Error Budget

For the following explorations, the large system assembly was culled down to just the mirror in the structural model. A reduced but representative thermal problem used just the mirror surrounded by its local heater can and the far field cold walls.

The mirror face deformations were studied as a function of mesh density by solving a uniform 10C temperature rise on 3 progressively finer meshes. The first mesh was the coarsest that could be tolerated in a model that might result from the larger system assembly and the finest mesh was expected to be the limit of computational affordability in a large system model.

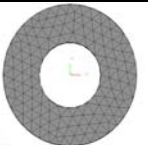
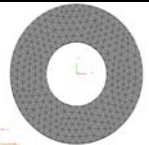
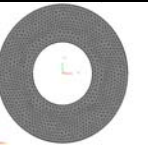
Face Displacement	Size 30	Size 20	Size 10
Min normal displacement	4.520E-6	3.074E-6	2.277E-6
Max normal displacement	7.160E-6	9.120E-6	9.651E-6
Ave normal displacement	6.313E-6	6.314E-6	6.305E-6
Number of Nodes	6508	13387	64915
Number of Elements	3296	7014	38921
			

Table 3. Mesh vs. Displacement

The change between the two finest meshes might be taken as a sensitivity coefficient representing change in solution quality with mesh refinement. With these three mesh samples, the solution appears to be converging. Mesh

convergence algorithms^{7, 8} could possibly shed light on remaining accuracy achievable with more mesh, but the finest mesh is nearly all that is computationally affordable without further trades. The error budget would have to cover this if the mesh density could not be increased. For example, other elements of the budget and sensitivity tree relate a distortion increment to a wavefront error and ultimately a portion of the requirement error. If the mesh-related errors don't significantly drive the front face average normal displacement, the OPD won't be strongly impacted. Mesh-related errors in other spatial components of the face, and therefore wavefront, distortion don't as strongly impact the OPD metric. This is a characteristic of interferometers and might not be the case for imaging systems.

Beyond mesh effects, the engineering understanding that spatially varying temperatures distorted the mirror needed to be grounded both to guide the design and to guide the simulation investment. The mirror distortion was studied under 3 additional temperature fields depicting linear variation in each individual coordinate direction. These, along with the uniform temperature, represent the first four components of a spatial decomposition of an arbitrary smoothly varying applied temperature field.

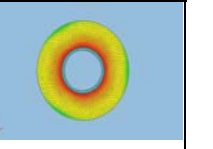
Entire Part	Uniform 10C	Linear X	Linear Y	Linear Z
Min Z displ	-7.146e-006	-8.876e-006	-8.690e-006	-4.512e-006
Max Z displ	7.310e-006	9.737e-006	1.046e-005	8.176e-006
Ave Z displ	2.583e-006	2.588e-006	2.580e-006	1.680e-006
				

Table 4. Displacement for Four Temperature Fields.

This information provides some clarity to the thermal modeling team concerning the resolution required on their computed temperature field and therefore their thermal mesh. In addition, these numerical trials provide cross discipline sensitivities that are at the core of the physics based error budget.

The mirror face distortions can be decomposed into Zernicke polynomials, formulated in a cylindrical coordinate system centered in the mirror face. These are commonly used for wavefront quality metrics. These coefficients are sensitivities of the optical metric to a spatial displacement pattern. For example, uniform normal displacement of the mirror face drives the piston optical metric while the lateral linear components drive tip and tilt. The uniform and linear temperature fields above produce these optical components. Cupping or curvature of the face drives optical power. A through-the-thickness temperature field, such as the linear-in-Z example above, was known to drive this component strongly.

Component	Uniform 10C	Linear X	Linear Y	Linear Z
Piston: 1	3.0691e-002	3.0692e-002	3.0677e-002	2.2960e-002
Tip: $2r \sin(\theta)$	-3.4036e-005	-2.9090e-005	9.3866e-003	-4.2923e-005
Tilt: $2r \cos(\theta)$	2.6004e-005	9.4213e-003	4.7686e-005	2.0297e-005
Astigmatism: $r^2 \sin(2\theta)$	7.2164e-005	6.3770e-005	4.3058e-004	6.3572e-005
Defocus: $2r^2 - 1$	1.0231e-002	1.0233e-002	1.0244e-002	2.0634e-003
Astigmatism: $r^2 \cos(2\theta)$	-6.0744e-005	-4.0673e-004	-6.9754e-005	-5.0950e-005

Table 5. Zernicke Distortion Components

In the thermal analyses, the mirror mesh density impacts the computed temperature field in several ways. The mirror heat balance is almost totally driven by radiation, but good assessment of conduction inside the mirror is needed to get accurate temperature across the mirror face (which drives optical distortion) and through the mirror thickness (which drives face curvature). Since the actual temperature fields are very smooth, spatially and temporally, the mesh density requirement is to capture local geometry primarily for thermal capacity. In addition, the standard practice is to use the same mesh density for radiation elements and the unprecedented accuracy requirement of 99+% capture of view factors leads to a very dense mesh.

From initial thermal balance studies, the relative importance of the far field temperatures was well understood. It was unclear however how much of the finer details, primarily in spatial variation, of the mirror's radiation context would be manifest in the mirror's temperature distributions. The cold plates of the far field walls were known to be

non-uniform but it wasn't clear how this would show up in the face distortions and the wavefront. Similarly, the mirror heater can was actively controlled and, because of its close thermal coupling to all sides of the mirror except the face, it was very effective in maintaining a uniform heat load. It wasn't clear, however, how the temporal deviations in the heater power controller would be manifested in the temporal components of the wavefront error.

	Minus 10%	Nominal	Plus 10%
Minimum	1.325E-6	1.472E-6	1.620E-6
Maximum	7.358E-6	8.176E-6	8.993E-6
Avg	4.568E-6	5.075E-6	5.583E-6

Table 6. Mirror Face Displacement vs Coefficient of Thermal Expansion

By the end of the test program, an intensive investigation into the contributions of the mirror coefficient of thermal expansion to the error led to an understanding of the spatial variation in the mirror blank. After coupon tests and model fitting efforts, a complex layered and asymmetric distribution of this critical material property was used. Prior to the testing, however, all that was known was that the face distortions were very sensitive to this parameter. Simple numerical tests such as shown in Table 6 above could have established a sensitivity for use in budgeting.

In the face of the above factors, a composite error budget is required. One branch would reflect the physics impacts as shown above. Another branch must allocate error terms to such numerical elements as mesh density and field representations. This directly exposes the sensitivities needed for budgeting work.

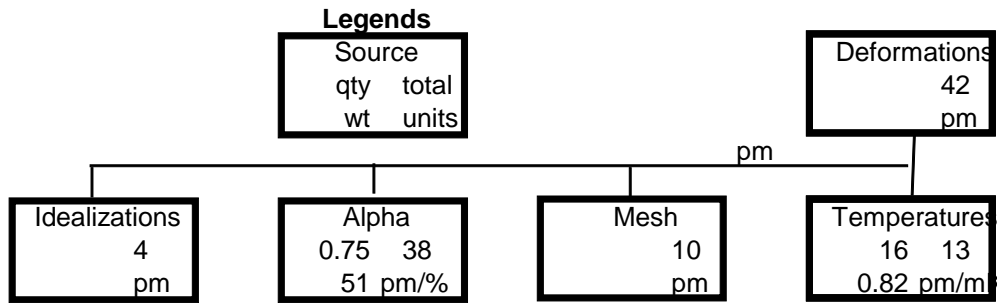


Figure 10. A Composite Error Budget Branch

Fig. 10 above composes several factors that impact the accuracy of the computed deformations. Clearly the temperature fields, or more relevant to an error budget, the temperature field errors, contribute to deformation errors. This sensitivity coefficient is based on the maximum face normal displacement produced by the linear-in-Z temperature field. The figure shows mesh errors, such as those discussed above resulting from a coarse mesh, and material property errors. The mesh error has been allocated 10 pm, where the mesh studies suggest the finest mesh above has on the order of 9 pm error in it. The coefficient of thermal expansion, alpha, receives the majority of the 42 pm total budget, but it is so sensitive that the required error of less than 1% is unlikely to be met. Other sources of error, not discussed, include approximations in the modeling of the mirror support struts which can cause rigid body motion errors.

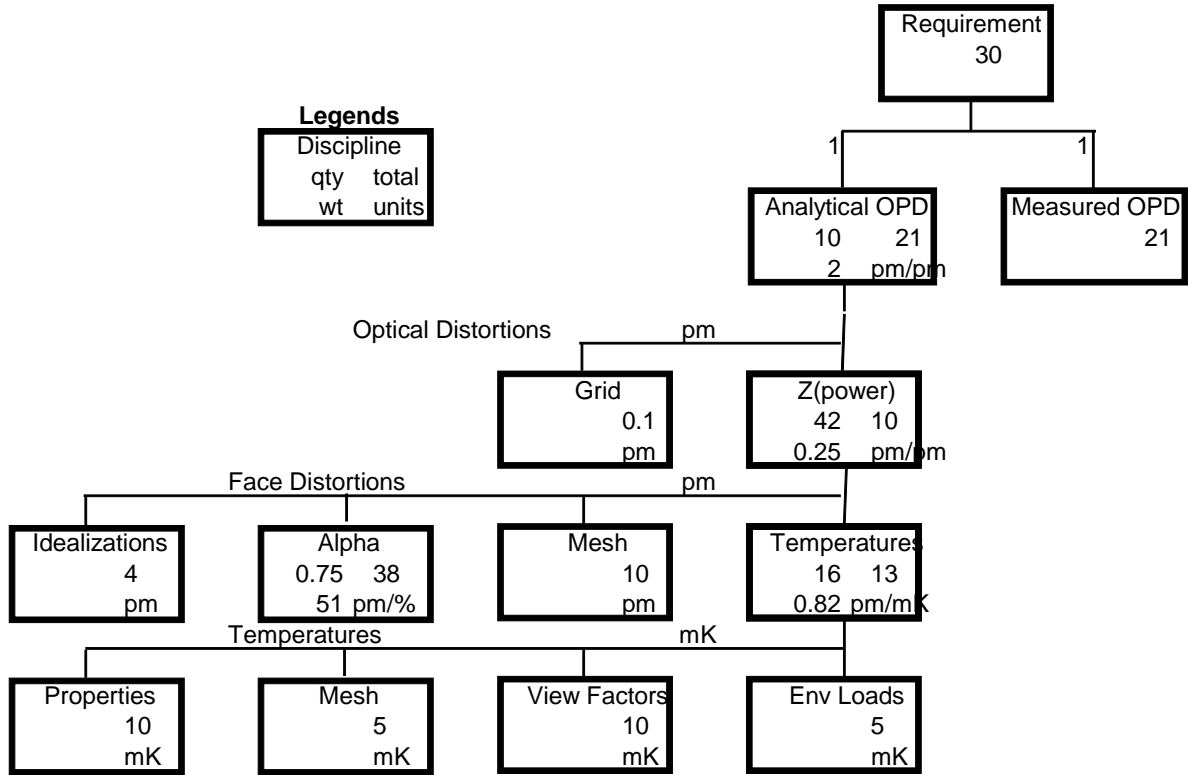


Figure 11. A Candidate Composite Error Budget

The composite error budget then looks like Fig. 11 above. Each tree level represents a sequential discipline in the “bucket brigade” reflecting the engineering understanding of the physics. The error allocations in that level are in units of the discipline. These are combined to drive the next level in RSS and multiplied by the sensitivity.

For example, at the structural modeling level, the errors in the prior temperature solution reflect contributions from the thermal problem inputs (heat loads) as well as the thermal modeling error expressed in terms of error in the temperature. This RSS temperature error is represented at the structural level as a distortion error through a sensitivity such as developed in the earlier discussions.

VII. Discussion

Although this composite budget invokes the underlying physics, it has substantial simplifications and judgments. To a good extent, this is a fair criticism of many error budgets which are often more “allocation” than “cause and effect.” A balanced view sees such a budget as a tool to guide subsequent imperfect efforts and balance choices toward the optimal.

Although many elements of this composite error budget look reasonable, the tight tolerance on the coefficient of thermal expansion cannot be achieved. Relief should be sought first in better fitting the sensitivity coefficient to the circumstance. The example used the average face displacement to a uniform temperature increase, but the linear-in-Z temperature field would be more appropriate. Still, this tight allocation might warrant early investigation into the material behavior. This would have given the project a significant advantage over finding it later when analyzing discrepancies with the measurements.

The example problem is reasonably complex. It involves several analytical and experimental engineering disciplines and an intricate and high precision product assembly. In some high-value project contexts, a substantially more elaborate tree might be warranted. The flight system has as many as ten such complex assemblies and each has a different impact on the optical performance. Other modeling aspects not discussed here, such as thermal controllers and maneuver models, might be explicitly represented.

VIII. Guiding the Investment

The error budget and weights are needed before the analysis models are built so that they can guide the investment in targeted portions of the model. Methods that are independent of the particular model and application are needed for this. Other methods, such as numerical derivatives, utilize an existing or similar working model and are useful in later stages of model application.

New rigor in model development and verification in support of flight systems will need this capability.²² Hardware development processes that call for a model development and management plan will expect such a rational basis for allocating funding and schedule resources to building the model. The error budget will also be an essential guide to experimental validation testing. Model components with high sensitivities or high budget weights are prime candidates for early risk reduction testing.

As a particular discipline team begins its assignment, representative but compact exploratory models might be constructed to test the assigned allocation and explore the modeling problem statement. Given fixed, limited and shared budget resources, the team needs to balance simplification and approximation against the breadth, quantity and volume of the modeling. By analogy to performance error budget rebalancing, a team that unexpectedly finds a high investment, sensitive area could request either a re-allocation to their branch or additional resources in relief. In the example problem here, the thermal coefficient of expansion in the mirror was such an unexpected case.

IX. Conclusion

Like any design activity, developing a modeling error budget will be iterative. Some notions of relative importance are needed before work starts and before a set of models is in hand. A simple allocated budget might suffice. Obvious critical, or poorly understood, areas might be explored with initial models. In the end, the budget will reflect the relative emphasis applied to completed work. A multidisciplinary model, such as this, is a complex entity and, while the laws of physics are clearly present, much of the cause and effect are obscured.

X. Acknowledgments

This research was carried out at the Jet Propulsion Laboratory, California Institute of Technology, under a contract with the National Aeronautics and Space Administration.

Reference herein to any specific commercial product, process, or service by trade name, trademark, manufacturer, or otherwise, does not constitute or imply its endorsement by the United States Government or the Jet Propulsion Laboratory, California Institute of Technology.

XI. References

1. Briggs, H.C., and Knutson, K, "Integrated Modeling and Analysis Using TeamCenter Engineering," PLMWorld 2005, Dallas, TX, 2-5 May, 2005.
2. Briggs, H.C., Phillips, C.J., and Orzewalla, M.A, "Integrated Modeling of Advanced Opto-Mechanical Systems," 47th AIAA/ASME/ASCE/AHS/ASC Structures, Structural Dynamics & Materials Conference, Newport, Rhode Island, 1 - 4 May 2006.
3. Lindensmith, C.A.; Briggs, H.C.; Beregovski, Y; Fera, V.A.; Goullioud, R.; Gursel, Y.; Hahn, I.; Kinsella, G.; Orzewalla, M.; Phillips, C.; Development and Validation of High Precision Models for SIM Planetquest," Proceedings of the 2006 IEEE Aerospace Conference, Big Sky, MT, 4-11 March, 2006.
4. Hemez, Francois M., "Challenges to the State-of-the-practice of Solution Convergence Verification," Paper AIIA-2007-1932, 48th AIAA/ASME/ASCE/AHS/ASC Structures, Structural Dynamics, and Materials Conference, 23 - 26 April 2007, Honolulu, HI.
5. Fraccone, G.Calanni, Ruzzene, M., Volovoi, V., Cento, P., Tibbals, T., and Vining, C., "Investigation of Sources of Uncertainty for Stress Prediction in Dynamic Structures," Paper AIAA-2007-1958, 48th AIAA/ASME/ASCE/AHS/ASC Structures, Structural Dynamics, and Materials Conference, 23 - 26 April 2007, Honolulu, HI.
6. Ghanem, R., Red-Horse, J., Benjamin, A., Doostan, A., and Zou, Y., "Stochastic Process Model for Material Properties Under Incomplete Information," Paper AIAA-2007-1968, 48th AIAA/ASME/ASCE/AHS/ASC Structures, Structural Dynamics, and Materials Conference, 23 - 26 April 2007, Honolulu, HI.
7. Roache, P.J., "Perspective: A Method for Uniform Reporting of Grid Refinement Studies," ASME Journal of Fluids Engineering, Vol. 116, September 1994, pp. 405-413.
8. Roache, P.J., "Verification of Codes and Calculations," AIAA JOURNAL Vol. 36, No. 5, May 1998.
9. Richardson, L. F., "The Approximate Arithmetical Solution by Finite Differences of Physical Problems Involving Differential Equations with an Application to the Stresses in a Masonry Dam," Transactions of the Royal Society of London, Series A, Vol. 210, 1910, pp. 307-357.

10. Loeven, G.J.A., Witteveen, J.A.S., and Bijl, H., "Efficient Uncertainty Quantification in Computational Fluid-Structure Interactions," Paper AIAA-2006-1634, 47th AIAA/ASME/ASCE/AHS/ASC Structures, Structural Dynamics, and Materials Conference, 1 -4 May 2006, Newport, RI.
11. Adhikari, S., "A Non-parametric Approach for Uncertainty Quantification in Elastodynamics," Paper- 2006-1630, 47th AIAA/ASME/ASCE/AHS/ASC Structures, Structural Dynamics, and Materials Conference, 1 -4 May 2006, Newport, RI.
12. Huyse, L., Thacker, B.H., Riha, D.S., Fitch, S.H.K., Pepin, J., and Rodriguez, E.A., "A Probabilistic Treatment of Expert Knowledge and Epistemic Uncertainty in NESSUS," Paper-2006-1830, 47th AIAA/ASME/ASCE/AHS/ASC Structures, Structural Dynamics, and Materials Conference, 1 -4 May 2006, Newport, RI.
13. Thacker, B.H., "The Role of Nondeterminism in Computational Model Verification and Validation," Proc. AIAA/ASME/ASCE/AHS/ASC 46th Structures, Structural Dynamics, and Materials (SDM) Conf, Austin, TX, April 2005.
14. Mullin, S.A., Walker, J.D., Riha, D., Thacker, B.H., Rodriguez, E.A., and Leslie, P.O., "Verification and Validation of a Penetration Model for the Design of a Blast Containment Vessel Part 1: Validation Experiments," Paper-2006-1919, 47th AIAA/ASME/ASCE/AHS/ASC Structures, Structural Dynamics, and Materials Conference, 1 -4 May 2006, Newport, RI.
15. Rodriguez, E.A., Pepin, J.E., Riha, D.S., Thacker, B.H., Fleming, J.B., and Walker, J.D., "Verification and Validation of a Penetration Model for the Design of a Blast Containment Vessel Part II: Model Validation," Paper-2006-1920, 47th AIAA/ASME/ASCE/AHS/ASC Structures, Structural Dynamics, and Materials Conference, 1 -4 May 2006, Newport, RI.
16. Hasselman, T., Lloyd, G., Hinnerichs, T., O'Gorman, C., and Urbina, A., "Validation of Uncertainty Quantification for Structures with Encapsulated Epoxy Foam," Paper-2006-1922, 47th AIAA/ASME/ASCE/AHS/ASC Structures, Structural Dynamics, and Materials Conference, 1 -4 May 2006, Newport, RI.
17. Logan, R.W., Nitta, C.K., and Chidester, S.K., "Uncertainty Quantification During Integral Validation: Estimating Parametric, Model Form, and Solution Contributions," Paper-2006-1923, 47th AIAA/ASME/ASCE/AHS/ASC Structures, Structural Dynamics, and Materials Conference, 1 -4 May 2006, Newport, RI.
18. Sarkar, A. and Ghanem, R., "Sensitivity Analysis of Stochastic Systems," Paper-2006-1988, 47th AIAA/ASME/ASCE/AHS/ASC Structures, Structural Dynamics, and Materials Conference, 1 -4 May 2006, Newport, RI.
19. Romero, V.J., "Some Issues and Needs in Quantification of Margins and Uncertainty in Complex Coupled Systems," Paper-2006-1989, 47th AIAA/ASME/ASCE/AHS/ASC Structures, Structural Dynamics, and Materials Conference, 1 -4 May 2006, Newport, RI.
20. B. F. Blackwell, K. J. Dowding, R. J. Cochran, and D. Dobranich, "Utilization of Sensitivity Coefficients to Guide the Design of a Thermal Battery," Proceedings of ASME Heat Transfer Division, HTD-Vol. 361-5, pp. 73-82, 1998.
21. Goullioud, R., Lindensmith, C.A., and Hahn, I., "Results from the TOM3 Testbed: Thermal Deformation of Optics at the Picometer Level," Proceedings of the 2006 IEEE Aerospace Conference, Big Sky, MT, 4-11 March, 2006.
22. H.C. Briggs, "Managing Analysis Models in the Design Process," Paper AIAA-2007-2268, 48th AIAA/ASME/ASCE/AHS/ASC Structures, Structural Dynamics, and Materials Conference, 23 - 26 April 2007, Honolulu, HI.